

# Epidemic extinction and control in heterogeneous networks

Jason Hindes<sup>1</sup> and Ira B. Schwartz<sup>1</sup>

<sup>1</sup>*U.S. Naval Research Laboratory, Code 6792, Plasma Physics Division,  
Nonlinear Dynamical Systems Section, Washington, DC 20375*

We consider epidemic extinction in finite networks with broad variation in local connectivity. Generalizing the theory of large fluctuations to random networks with a given degree distribution, we are able to predict the most probable, or optimal, paths to extinction in various configurations, including truncated power-laws. We find that paths for heterogeneous networks follow a limiting form in which infection first decreases in low-degree nodes, which triggers a rapid extinction in high-degree nodes, and finishes with a residual low-degree extinction. The usefulness of the approach is further demonstrated through optimal control strategies that leverage finite-size fluctuations. Interestingly, we find that the optimal control is a mix of treating both high and low-degree nodes based on large-fluctuation theoretical predictions.

PACS numbers: 89.75.Hc, 05.40.-a, 87.10.Mn, 87.19.X-

Extinction of epidemics in finite networks is an important topic in population dynamics [1, 2]. Though many factors may contribute, such as environmental changes and social behavior, it has been demonstrated, and rigorously proven for finite populations, that internal fluctuations in a system's dynamics can organize in special ways over long time-scales to drive infections to zero [3–5]. Such fluctuations to infection-free states have been studied extensively in well-mixed systems, including the role of vaccination and treatment programs in reducing the average time to extinction [3, 6]. Moreover, the effects of local transmissions on the most probable, or optimal path to extinction have been considered for homogeneous networks having a finite average degree [7].

Somewhat separately, much work has been done in characterizing the deterministic dynamics, epidemic threshold, outbreak size distributions, small fluctuations, and Griffiths phases of epidemics in complex networks [8–14]. Only very recently has there been progress in understanding the interplay between stochastic noise and network dynamics that can lead to large fluctuations and switching between states [15]. However, very little is known about how internal noise inherent to epidemic extinction pertains in heterogeneous networks having vastly differing topologies.

In this letter we construct and analyze the most probable path through heterogeneous networks to extinction. Novel in this work, is that we show the path has two primary forms, close-to and far-from the epidemic threshold. In the latter, we demonstrate an interesting multi-step structure in which low-degree node infections decrease first, followed by a quick, nearly complete extinction in high-degree nodes, and finishing with a low-degree extinction. The approach is then used to find targeted optimal treatment strategies that can exponentially reduce extinction times, but do not trivially treat the most well connected nodes nor minimize the epidemic size. Control that specifically manipulates finite-size fluctuations inherent in contact processes is also novel in the study of

complex networks [6, 15].

To understand how extinctions depend on topological heterogeneity, we consider the stochastic SIS model on random networks, both quenched and annealed, with a given degree distribution,  $g_k$ , where the degree,  $k$  is the number of links of a node. The former can be constructed with the configuration model (*CMN*), by first generating nodes, each with a number of edge “stubs” drawn from  $g_k$ , and then connecting pairs of “stubs” to form links, chosen uniformly at random [16]. The adjacency matrix,  $A$ , for such a network, is defined such that,  $A_{ij}$ , is 1 if nodes  $i$  and  $j$  are linked, and 0 otherwise. In the latter, the network is assumed to fluctuate rapidly with respect to the SIS dynamics such that  $A$  is given by the weighted average of *CMNs* [8, 9, 14].

For SIS dynamics on a general network, node  $i$  is either infected, denoted  $\nu_i = 1$ , or susceptible,  $\nu_i = 0$ , and changes its state  $\nu_i : 0 \rightarrow 1$  with probability per unit time  $\beta(1 - \nu_i) \sum_j A_{ij} \nu_j$ , and  $\nu_i : 1 \rightarrow 0$  with probability per unit time  $\alpha \nu_i$ , where  $\beta$  and  $\alpha$  are known as the infection and recovery rates, respectively. In order to describe the dynamics given these reactions, it is useful to approximate  $A$  with the annealed limit, in which  $A_{ij}$  approaches the probability that nodes  $i$  and  $j$  are neighbors, and is proportional to the product of their degrees,  $k_i k_j$ , or  $A_{ij} \approx k_i k_j / (N \langle k \rangle)$ . This is known as the annealed network approximation and represents a mean-field for heterogeneous networks [8, 9]. Given this form, the state of the network can be described by the number of infected nodes with degree  $k$ ,  $I_k$ , which has corresponding reactions and rates:  $I_k \rightarrow I_k + 1$  with rate of infection  $w_k^{inf}(\mathbf{I}) = \beta k (N_k - I_k) \sum_{k'} k' I_{k'} / (N \langle k \rangle)$ , and  $I_k \rightarrow I_k - 1$  with recovery rate  $w_k^{rec}(\mathbf{I}) = \alpha I_k$ , where  $\mathbf{I}_k = \langle I_{k1}, I_{k2}, \dots, I_{k_{max}} \rangle$ , and  $N_k = g_k N$ .

Thus, the probability distribution  $\rho(\mathbf{I}, t)$  for the *SIS* model on networks having a general degree distribution

satisfies an approximate master equation:

$$\begin{aligned} \frac{\partial \rho}{\partial t}(\mathbf{I}, t) &= \sum_k w_k^{inf}(\mathbf{I} - \mathbf{1}_k) \rho(\mathbf{I} - \mathbf{1}_k, t) - w_k^{inf}(\mathbf{I}) \rho(\mathbf{I}, t) \\ &+ w_k^{rec}(\mathbf{I} + \mathbf{1}_k) \rho(\mathbf{I} + \mathbf{1}_k, t) - w_k^{rec}(\mathbf{I}) \rho(\mathbf{I}, t), \end{aligned} \quad (1)$$

where  $\mathbf{1}_k = \langle 0_{k1}, 0_{k2}, \dots, 1_k, \dots, 0_{kmax} \rangle$ .

It is known that for sufficiently large  $N$ , Eq.(1) possesses quasi-stationary solutions about an endemic state with long-lived infection that decays into an extinct state over exponential time-scales [18, 19]. We therefore approximate such solutions with a *WKB* ansatz; i.e., assume  $\rho(\mathbf{I}, t) = e^{-NS(\mathbf{x}, t)}$ , where  $\mathbf{x} = \mathbf{I}/N$ , and take  $w_k(\mathbf{I} \pm \mathbf{1}_k) \approx w_k(\mathbf{I})$  and  $\rho(\mathbf{I} \pm \mathbf{1}_k, t) \approx e^{-NS(\mathbf{x})} e^{\mp \partial S / \partial x_k}$ . This gives a Hamilton-Jacobi equation,  $\frac{\partial S}{\partial t} + H(\mathbf{x}, \frac{\partial S}{\partial \mathbf{x}}) = 0$ , where  $S$  and  $H$  are called the action and Hamiltonian, respectively. The latter is a function of the coordinate,  $\mathbf{x}$ , and the conjugate momentum,  $p_k = \partial S / \partial x_k$ :

$$H(\mathbf{x}, \mathbf{p}) = \sum_k \left[ \beta k (g_k - x_k) (e^{p_k} - 1) \sum_{k'} \frac{k' x_{k'}}{\langle k \rangle} + \alpha x_k (e^{-p_k} - 1) \right]. \quad (2)$$

We analyze Eq.(3) by solving the canonical equations of motion:  $\dot{x}_k = \partial H / \partial p_k$ ,  $\dot{p}_k = -\partial H / \partial x_k$ , in terms of the fraction of each degree class infected,  $y_k = x_k / g_k$ , the ratio  $\beta / \alpha = \tilde{\beta}$ , and the re-scaled time,  $\tau = \alpha t$ :

$$\begin{aligned} \dot{y}_k &= \tilde{\beta} k (1 - y_k) e^{p_k} \sum_{k'} \frac{k' g_{k'}}{\langle k \rangle} y_{k'} - y_k e^{-p_k}, \quad (3) \\ \dot{p}_k &= \tilde{\beta} k \sum_{k'} \frac{k' g_{k'}}{\langle k \rangle} \left[ y_{k'} (e^{p_k} - 1) - (1 - y_{k'}) (e^{p_{k'}} - 1) \right] - e^{-p_k} + 1. \end{aligned}$$

For the quasi-stationary distribution,  $\frac{\partial S}{\partial t} = H = 0$ , the optimal path from the endemic state to extinction is one that extremizes the action:

$$S = \int [\mathbf{p} \cdot \dot{\mathbf{x}} - H] dt = \sum_k g_k \int p_k dy_k, \quad (4)$$

with the average time to extinction scaling as  $\langle T \rangle \sim e^{NS}$ . The path is a heteroclinic orbit connecting two equilibria of Eq.(3): from an endemic fixed-point,  $y_k^* = 1 / (1 + 1 / (Y \tilde{\beta} k))$ ,  $p_k = 0$ , to extinction with non-zero momentum,  $y_k = 0$ ,  $p_k^* = -\ln(1 + \tilde{\beta} k (1 - P))$  [3, 5, 17]. The functions  $Y$  and  $P$  depend on  $\tilde{\beta}$ , with  $(Y, P) \rightarrow (0, 1)$  as  $\tilde{\beta} \langle k^2 \rangle / \langle k \rangle \equiv R_0 \rightarrow 1$ , and  $(Y, P) \rightarrow (1, 0)$  as  $\tilde{\beta} \rightarrow \infty$ . Fig.(1) shows comparisons between projections of pre-history trajectories to extinction from stochastic simulations and optimal paths of Eq.(3) for several network configurations computed with the iterative action minimizing method (IAMM) [20].

Qualitatively, we find two important parameter regions to consider. First, close to the epidemic threshold when  $R_0 - 1 \gtrsim 0$  (which we call ‘‘weak’’), the paths to extinction are approximately linear from  $(y_k^*, 0)$  to  $(0, p_k^*)$ .

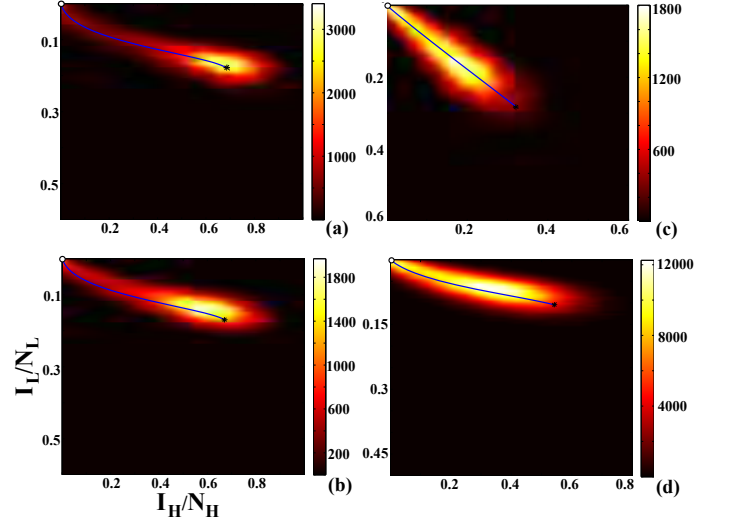


FIG. 1: Density (unnormalized) of 1000 simulations projected into the fraction of infected high (H) and low-degree (L) nodes. Predicted paths are shown in blue from the endemic state(\*) to extinction(o). (a) annealed network with  $N = 300$  and  $\tilde{\beta} = 0.096$ , and two degree classes,  $k \in \{5, 50\}$ , with  $k=50$ -nodes occupying 10% of the network. (b) a corresponding *CMN*. (c) a *CMN* with  $N = 350$ ,  $\tilde{\beta} = 0.092$ , and  $g_k = e^{-16} 16^k / k!$  where high-degree nodes have  $16 \leq k \leq 18$ , and low-degree have  $13 \leq k \leq 15$ . (d) a *CMN* with  $N = 600$ ,  $\tilde{\beta} = 0.038$ , and  $g_k = k^{-2.5} / \sum_{k'=10}^{300} k'^{-2.5}$  where high-degree nodes have  $70 \leq k \leq 235$ , and low-degree have  $10 \leq k \leq 12$ .

The explicit form can be seen by expanding the equilibria in powers of  $R_0 - 1$ , which gives to first order,  $y_k^* \approx k \langle k^2 \rangle (R_0 - 1) / \langle k^3 \rangle = -p_k^*$ , implying that the endemic state and momentum at extinction are simply proportional to degree when the infection is weak. This is intuitive since in the weak limit high-degree nodes drive the epidemic, when only their local reproductive numbers are sufficient to spread infection, ( $\beta k > 1$ ), and therefore must recover disproportionately without reinfection in order for extinction to occur. Paths near the weak limit can be seen in Fig.1(b) and (d) where  $R_0 = 1.6$  and  $R_0 = 2.0$  respectively, and in Fig.2(a)-(red).

Also for weak infection, the action along the path from Eq.(4) is therefore:

$$S_{weak} = \frac{\langle k^2 \rangle^3}{2 \langle k^3 \rangle^2} (R_0 - 1)^2 + \mathcal{O}(R_0 - 1)^3, \quad (5)$$

which depends on the distance from the epidemic threshold and an additional topological factor that generally decreases with increased broadness in the degree distribution. In contrast, in the well-mixed limit (or homogeneous complete graph) the action only depends on  $R_0$  [21]. The predicted reduction in extinction times with topological fluctuations is intuitive, since for very heterogeneous networks only a small fraction of highly connected nodes must recover without reinfection, compared

with most nodes for homogeneous networks.

On the other hand if most nodes can propagate infection,  $\tilde{\beta}\langle k \rangle \gg 1$  (which we call “strong”), then the interplay between degree classes and the path to extinction are more complicated as the global dynamical structure of the path becomes apparent. However, we find that a limiting form emerges when comparing the dynamics of low and high-degree nodes by which the path can be described in multiple steps.

Because in the strong limit most nodes will be infected in the endemic state, it is very improbable that high-degree nodes can recover without being reinfected, and thus we expect infection must first disproportionately decrease in low-degree nodes. We can extract the form of this step, by analyzing the unstable eigen-mode of the endemic equilibrium:  $(y_k, p_k) = (y_k^* + \epsilon_k^{(1)}, \mu_k^{(1)})$ , to linear order and studying the asymptotic scaling of  $(\epsilon_k^{(1)}, \mu_k^{(1)})$  for large  $\tilde{\beta}k$ . Inserting these assumptions into Eq.(3), we find that  $(\epsilon_k^{(1)}, \mu_k^{(1)})$  must satisfy an eigenvalue equation for the rate  $\lambda^{(1)}$ :

$$\left[ \lambda^{(1)} + 1 + \frac{k(\tilde{\beta}\langle k \rangle - 1)}{\langle k \rangle} \right] \epsilon_k^{(1)} - \left[ 2 - \frac{1}{\tilde{\beta}k} - \frac{1}{\tilde{\beta}\langle k \rangle} \right] \mu_k^{(1)} \approx \sum_{k'} \frac{k' g_{k'}}{\langle k \rangle} \epsilon_{k'}^{(1)}.$$

Since  $\lambda^{(1)}$  and the sum are  $k$ -independent, it must be that for large  $\tilde{\beta}k$ , we have  $\epsilon_k^{(1)}/\epsilon_{k'}^{(1)} \sim k'/k$  (the relative decrease in infection shown in Fig.2(b)-(1)), with relative momenta initially tending to a constant.

In the second step (Fig.2(b)-(2)), the small build-up of momenta for high-degree nodes becomes rapid as two oppositely signed contributions to the force in  $\dot{p}_k$  (Eq.(3)) approach a minimum along the path:

$$F_k = \sum_{k'} \frac{k' g_{k'}}{\langle k \rangle} \left[ y_{k'} (e^{p_k} - 1) - (1 - y_{k'}) (e^{p_{k'}} - 1) \right] \rightarrow \min[F_k],$$

which quickly pushes  $-p_k$  toward its maximum  $-p_k^*$ . Also, we can see from Eq.(3) that only when  $-p_k$  is large does  $y_k$  decrease significantly, implying that  $y_k$  remains near the endemic state until the large momentum of this step is reached. This suggests that we can approximate the average speed of step-two with the upper bound of the maximum possible speed,  $\max[-\dot{y}_k] \lesssim y_k^* e^{-p_k^*}$  giving the scaling for large  $\tilde{\beta}k$ :  $\epsilon_k^{(2)}/\epsilon_{k'}^{(2)} \sim k/k'$ .

In the last step (Fig.2(b)-(3)), we expect to have a final decrease in low-degree node infections in a background of very small numbers of infected high-degree nodes, since the latter were rapidly depleted in the second step. The scaling can be found by analyzing the extinct state's stable eigen-mode:  $(y_k, p_k) = (\epsilon_k^{(3)}, p_k^* + \mu_k^{(3)})$ , which gives an eigenvalue equation for the rate  $\lambda^{(3)}$ ,

$$\left[ 1 + \frac{1}{\tilde{\beta}k} - \frac{1}{\tilde{\beta}\langle k \rangle} \right] \left[ \lambda^{(3)} + 1 + \frac{k(\tilde{\beta}\langle k \rangle - 1)}{\langle k \rangle} \right] \epsilon_k^{(3)} \approx \sum_{k'} \frac{k' g_{k'}}{\langle k \rangle} \epsilon_{k'}^{(3)},$$

that in the limit of large  $\tilde{\beta}k$  implies  $\epsilon_k^{(3)}/\epsilon_{k'}^{(3)} \sim k'/k$ . Examples are shown in Fig.2(a)(black) and Fig.2(b)(black); in the former, the strong limit scaling starts to be visible for  $R_0 \gtrsim 3$ . Also, Fig.2(a) shows the significant qualitative difference between the epidemic path toward the endemic state (green), which has been well studied, and the optimal path to extinction [9].

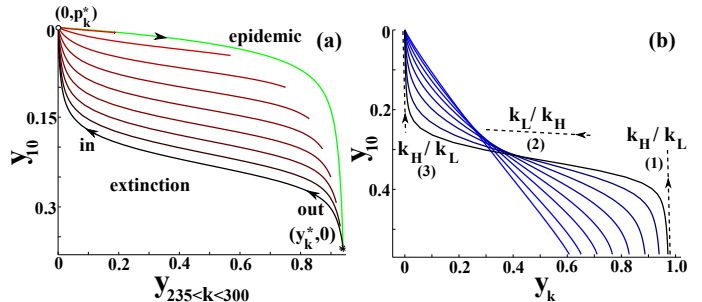


FIG. 2: (a) Projections of the optimal paths for truncated power-law (see Fig.1(d)) shown for increasing  $R_0 \in [1.1, 5.1]$  (red→black, weak→strong) in steps of 0.5, compared with the path into the endemic state for  $R_0=5.1$  (green). Arrows indicate direction in time. (b) Projections into  $y_k$  for the same distribution with  $R_0=9$  and 17 bins[23], shown for bins with increasing  $k$ :  $\{k=12, 14 \leq k \leq 15, 18 \leq k \leq 20, 24 \leq k \leq 27, 34 \leq k \leq 41, 53 \leq k \leq 69, 97 \leq k \leq 143, 236 \leq k \leq 300\}$  (blue→black), and compared with the predicted scaling for the highest bin (dashed lines).

In addition to a theoretical interest in the geometry of the optimal path, it is also practically interesting, since the network's extinction times will scale exponentially with its action [18, 19]. Therefore, we suggest the action can provide a measure for the effectiveness of optimal epidemic control strategies in finite networks [6]. We illustrate the approach with a random treatment procedure for infected nodes with degree  $k$ , such that they recover with an increased rate,  $\gamma w_k$ , where  $\gamma$  is the overall treatment rate, and  $w_k$  is a targeting fraction of the infected population:  $\sum_k w_k = 1$ .

In the weak limit we expect optimal treatment to be dominated by large  $k$  (similar to targeted immunization), since  $y_k^*$  and  $p_k^*$  are proportional to  $k$  [22]. However in the strong limit, treating low-degree nodes close to  $\langle k \rangle$  will tend to decrease  $S$ , since their numbers must be lowered in the first step, before momenta differ significantly from zero. In intermediate cases, we expect a mixed strategy to minimize the action. Treatment results are shown in Fig.3 for a simple bimodal network with two degree classes for clarity.

Interestingly, we find that choosing the optimal  $w_k$  for the bimodal network can result in a nearly %50 decrease in the action, implying an enormous reduction in extinction times, i.e.,  $\langle T \rangle \rightarrow \langle T \rangle^{1/2}$  (Fig.3-inset). Furthermore, we note that in Fig.3 the size of the endemic state is minimized when  $w_{50}=0$ , the equilibrium treatment rate,  $\gamma \sum_k w_k g_k y_k^*$ , is maximized when  $w_{50}=0$ , and  $R_0$  is min-

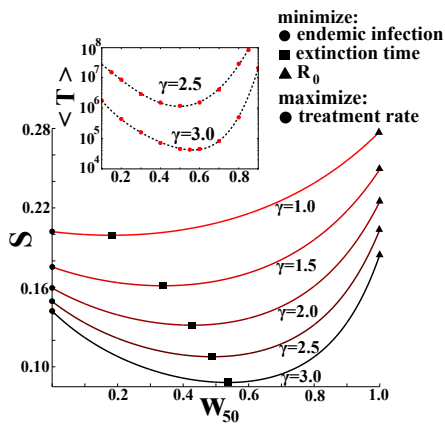


FIG. 3: Action versus the fraction of infected high-degree nodes treated in a bimodal network (see Fig.1(a)-(b)) and increasing treatment rate,  $\gamma$  (red $\rightarrow$ black):  $\beta = 0.275$ . The inset shows the extinction times for a CMN with  $N=200$ .

imized when  $w_{50} = 1$ , but none correspond to the minimum action control. The example demonstrates that designing optimal controls intended to drive epidemics to extinction in finite networks cannot be found from the intuitive results of the deterministic limit alone,  $p_k = 0$ . In particular, infection can be brought to zero through controls even when  $R_0 > 1$ .

In conclusion, we have considered how fluctuations in the SIS model produce extinctions from internal noise in finite heterogeneous networks, and found that the process is captured by a most probable path. We were able to construct paths by combining the theory of rare events and random networks with a general degree distribution, and predict important consequences, such as the exponential decrease in extinction times with topological variation, as well as the multi-step scaling of extinction through nodes with very different degree. Furthermore, we demonstrated how the theory can be used to leverage fluctuations for optimal network control, producing exponential decreases in extinction times with a simple treatment strategy based on action minimization. Our theoretically predicted results were confirmed by simulations over large parameter ranges and different network topologies.

Lastly, we suggest the theoretical approach can be tailored to more arbitrary weighted networks using spectral techniques and binning, which would allow one to predict the paths to extinction through real networks, and could be applied to more general epidemic processes [1, 8, 13, 24].

We are grateful to Luis Mier-y-Teran Romero, D. J. Schneider, B. S. Lindley, C. R. Myers, and L. B. Shaw for useful discussions. J. H. is a National Research Council postdoctoral fellow. I.B.S was supported by the U.S. Naval Research Laboratory fund-

ing (N0001414WX00023) and office of Naval Research (N0001414WX20610).

- 
- [1] R. M. Anderson and R. M. May, *Infectious Diseases of Humans* (Oxford University Press, 1991).
  - [2] J. R. Banavar and A. Maritan, *Nature* **460**, 334 (2009).
  - [3] M. I. Dykman, I. B. Schwartz, and A. S. Landsman, *Phys. Rev. Lett.* **101**, 078101 (2008).
  - [4] M. Khasin and M. I. Dykman, *Phys. Rev. Lett.* **103**, 068101 (2009).
  - [5] A. Kamenev, B. Meerson, and B. Shklovskii, *Phys. Rev. Lett.* **101**, 268103 (2008).
  - [6] L. Billings, L. Mier-y Teran-Romero, B. S. Lindley, and I. B. Schwartz, *PLoS One* **8**, e70211 (2013).
  - [7] B. S. Lindley, L. B. Shaw, and I. B. Schwartz, *Europhys. Lett.* **108**, 58008 (2014).
  - [8] R. Pastor-Satorras, C. Castellano, P. Van Mieghem, and A. Vespignani, *Rev. Mod. Phys.* **87**, 925 (2015).
  - [9] R. Pastor-Satorras and A. Vespignani, *Phys. Rev. Lett.* **86**, 3200 (2001).
  - [10] S. N. Dorogovtsev, A. V. Goltsev, and J. F. F. Mendes, *Rev. Mod. Phys.* **80**, 1275 (2008).
  - [11] M. E. J. Newman, *Phys. Rev. E* **66**, 016128 (2002).
  - [12] M. A. Muñoz, R. Juhász, C. Castellano, and G. Ódor, *Phys. Rev. Lett.* **105**, 128701 (2010).
  - [13] A. V. Goltsev, S. N. Dorogovtsev, J. G. Oliveira, and J. F. F. Mendes, *Phys. Rev. Lett.* **109**, 128702 (2012).
  - [14] E. Valdano, L. Ferreri, C. Poletto, V. Colizza, *Phys. Rev. X* **5**, 021005 (2015).
  - [15] D. K. Wells, W. L. Kath, and A. E. Motter, *Phys. Rev. X* **5**, 031036 (2015).
  - [16] M. E. J. Newman, *Networks: An Introduction* (Oxford University Press, 2010).
  - [17] V. Elgart and A. Kamenev, *Phys. Rev. E* **70**, 041106 (2004).
  - [18] M. I. Dykman, E. Mori, J. Ross, and P. M. Hunt, *J. Chem. Phys.* **100**, 5735 (1994).
  - [19] M. I. Friedlin and A.D. Wentzell, *Random Perturbations of Dynamical Systems* (Springer-Verlag, New York, 1998), 2nd ed..
  - [20] B. S. Lindley and I. B. Schwartz, *Physica D* **255**, 22 (2013).
  - [21] C.R. Doering, K. V. Sargsyan, and L. M. Sander, *Multi-scale Model. Simul.* **3**(2), 283 (2005).
  - [22] R. Pastor-Satorras and A. Vespignani, *Phys. Rev. E* **65**, 036104 (2002).
  - [23] Since the path is hyperbolic and power-laws have many degree classes, it is useful to apply a binning procedure that reduces the dimension for the IAMM. Above, we have uniformly binned the distribution  $kg_k/\langle k \rangle$ , and replaced  $k$  with the average in each bin. This was chosen because it gives accurate approximations for  $\langle k^2 \rangle / \langle k \rangle$ . Also,  $k_{max}$  was chosen small enough such that at least  $\mathcal{O}(1)$  nodes could be expected in its bin given  $N$ .
  - [24] Spectral approaches can provide quantitative improvements in accuracy [8, 13], e.g, in networks with large spectral gaps.